Possible planting boundaries of winter wheat in China under different emissions scenarios

Maowei Wu[1], Zhixin Hao[1,2 *], Yang Xu[1], Jingyun Zheng[1,2]

[1] Key Laboratory of Land Surface Pattern and Simulation, Institute of Geographic Sciences and Natural Resources Research, Chinese Academy of Sciences, Beijing 100101, China

[2] University of Chinese Academy of Sciences, Beijing 100049, China

Corresponding Author: Dr. and Prof. Zhixin Hao

Email: haozx@igsnrr.ac.cn

Institution: Institute of Geographic Sciences and Natural Resources Research, Chinese Academy of Sciences

Address: No 11A Datun Road, Chaoyang District Beijing 100101, China

Abstract

Suitable planting areas for winter wheat in north China are expected to shift northwardly due to climate change, however, the increasing extreme events and the deficiency of water supply are threatening the security of planting system. Thus, based on predicted climate data for 2021–2050 under the SSP1-2.6, SSP3-7.0, and SSP5-8.5 emission scenarios, as well as historical data from 1961–1990, we use four critical parameters of percentage of extreme minimum temperature occurrence, first day of the overwintering period (FD), sowing date (SD), and precipitation before winter (PBW) to determine the planting boundary of winter wheat. The results show that, the frequency of extreme minimum temperature occurrence is expected to decrease in the North winter wheat area, which will result in a northward movement of the western part of northern boundary by 73, 94, and 114 km on average, as well as FD delays ranging from 6.0 to 10.5 days. Moreover, the agrometeorological conditions in the Huang-Huai winter wheat area are expected to exhibit more pronounced changes than the rest of the studied areas, especially near the southern boundary, which is expected to retreat by approximately 213, 215, and 233 km northwardly. The north boundary is expected to move 90–140 km northward. Therefore, the change in southern and northern boundaries will lead the potential planting areas of the entire North winter wheat area to increase by 10,700 and 28,000 km^2 on average in the SSP3-7.0 and SSP5-8.5 scenarios but decrease 38,100 km^2 in the SSP1-2.6 scenario.

Key Points:

The potential changes in the northern and southern winter wheat cultivation boundaries during 2021-2050

The occurrence of extremely low-temperature years will decline in the North winter wheat area due to climate change

SD and FD, the two phenological stages before winter, are projected to be delayed in the forecasted period

. Introduction

Wheat is the third-largest crop in the world and provides 20% of human dietary protein and caloric intake globally (Shiferaw et al., 2013). Its broad adaptability to climatic conditions and variety diversity accounts for its unparalleled cultivation range, from 67°N in Scandinavia and Russia to 45°S in Argentina (Shewry and Hey, 2015). As stated by FAO, the production of wheat has increased from 218.5 million tons in 1961 to 732 million tons in 2013 (Tadesse et a l., 2016). Nonetheless, with the continually increasing global mean surface temperature since the Industrial Revolution (IPCC, 2021), climate change and increasing extreme climate events disturb the agricultural ecosystem and result in changes in local suitable agrometeorological conditions, affecting wheat growth. Therefore, wheat cultivation spatial distribution has shifted globally, with a general northward movement trend. For example, the hard red winter wheat in the 1980s extended twice the area than that in the 1920 in the North American, and the planting regions exhibited northward and northwestward shifts (Rosenberg, 1982). Thus, climate change is expected to substantially expand the suitable regions for winter wheat cultivation in North American northwardly into Canada and extend the fall-sown spring wheat region northwardly and eastwardly (Rosenzweig, 1985). In northern Europe, suitable areas for winter wheat cultivation have expanded almost into the Arctic Circle (66.5ºN) (Kenny et al., 1993). Crops in southern Europe, such as maize, sunflower, and soya beans, could also expand further north and occur at higher altitudes (Audsley et al., 2006; Olesen et al., 2007). Although warmer temperatures benefit wheat cultivation at high latitudes by reducing cold-temperature constraints on agricultural development, typical wheat planting areas in the tropics will be gradually reduced (Rosenzweig and Parry, 1994). Therefore, the negative impacts of climate change on global wheat production will likely become a critical issue to address in the future. As predicted by Balkovic et al. (2014), global wheat production at current conventional management methods would decrease under all RCPs by 37 to 52 Mt and by 54 to 103 Mt in the 2050s and 2090s, respectively.

China is the largest wheat producer in the world, possessing 11% of the global wheat cultivation areas and contributing to 17% of the global wheat production (USDA, 2016). Winter wheat accounts for more than 90% of the total wheat yields in China (National Bureau of Statistics of China, 2017). The winter wheat cultivation zone climatic indices in China are based on tolerable low temperatures for winter wheat growth (Zhao, 2010, Sun et al., 2013), as varying degrees of freeze damage during the overwintering stage may have different negative impacts on winter survival rate, crop vigor, and therefore final yields (Vico et al., 2014; Zheng et al., 2018). However, temperature change spatial distribution patterns in China exhibit a strong similarity to global changes, with temperature increases occurring in the entire region, albeit more noticeably in

the northern region (Guo et al., 2013). This northward expansion over the past few decades has been largely attributed to the longer growing seasons and decreased temperature-related constraints on crop growth that have resulted from warmer temperatures. Increasing attention has begun to focus on the changes in winter wheat cultivation distribution and possible planting boundaries in China, and substantial progress in the characterization of this phenomenon has been achieved. For instance, an observed significant relationship is that the sowing date is delayed for 4 days when the temperature increased by 1°C (Li Y. et al., 2013). The planting boundaries for different winter wheat varieties in China moved significantly northwardly in 1981-2010, compared to the 1951–1980 period (Li K. et al., 2013). Moreover, the overall potential planting areas for winter wheat increased as well. The strong winterness-variety winter wheat had the largest change in both the movement of the planting boundary and the planting area increase. Hao et al. (Hao et al., 2018) analyzed changes in suitable winter wheat planting boundaries along its production areas in China under the RCP4.5 scenario and predicted a northward shift of the northern winter wheat boundary by 1–2°N. Planting area has increased 1,420 km^2 in the year 2019 compared to that in the year 2000 by Landsat image mapping (Zhang et al., 2021).

So far, most previous studies have focused on the northern boundary shifts, rather than on those occurring in both the southern and northern boundaries in the coming decades. Moreover, some studies have been limited to the provincial or regional scale, and thus cannot represent the general impact of climate change on agriculture. Therefore, this study aimed to assess the impacts of climate change on agrometeorological index trends associated with wheat safe overwintering in the winter wheat region of China under low (SSP1-2.6), medium-high (SSP3-7.0), and high (SSP5-8.5) emission scenarios, as well as further to explore the potential wheat planting boundaries in the future. Thus, the findings of this study could provide reference for other agriculture planting regions and scientific data for climate change adaptation and responses in food security.

2. Materials and methods

2.1. Study area

The winter wheat planting region in China is divided into North winter wheat area and South winter wheat area border by by Huaihe River, based on the geographical environment, natural conditions, climatic factors, farming system and wheat varieties (Zhao, 2010). In this study, we focus on the North winter wheat area (I), which is located south of the Great Wall and north of the Huaihe River, and includes the Shandong, Henan, Hebei, Shanxi, Shaanxi, southeastern Gansu, and north part of Jiangsu and Anhui Provinces (Figure 1). Crops ripen twice per year or three times every two years (Hu et al., 2019; Li and Lei, 2021). The climatic conditions are suitable for winter or strong winter variety of winter wheat growing, with annual mean temperature of 9–15 °C, extreme minimum temperature of −30.0 to −13.2 °C from north to south, and the annual active accumulated temperature ranges of 2,750 to 4,900 °C. And North winter wheat

area can be divided into Northern winter wheat subregion (Ia) and Huang-Huai winter wheat subregion (Ib), according to latitudes, terrains, and climatic conditions. For the Ia, the winter wheat is sown at the end of September to early-October and harvested until mid-June to late-June, but for Ib, the sowing date is same as Ia, and the harvest time is advanced to early-June. In addition, since the possible winter wheat planting boundaries might move northward due to the climate warming, we also plot the spring winter wheat area (II) in the north of the north winter wheat area in Figure 1.

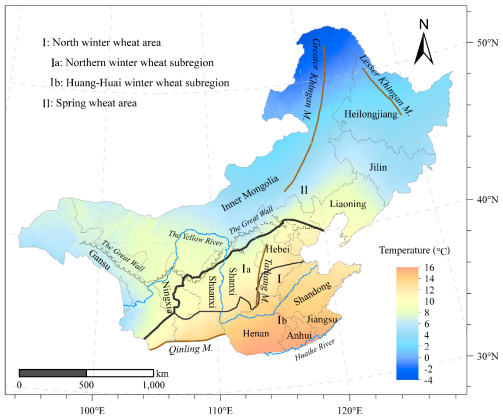

Figure 1. Map of north winter wheat area; Shaded colors indicate the temperature spatial pattern (mean value from 1991 to 2019), using daily meteorological dataset of basic meteorological elements of China National Surface Weather Station (V3.0)

2.2. Data

The Shared Socio-economic Pathways (SSPs) are five distinctly different scenarios by an international team of climate scientists, economists and energy systems modelers, and adopted by the Sixth Assessment Report of the Inter-

governmental Panel on Climate Change, which describe how global societies, populations, and economies will change under the context of climate change adaptation and mitigation (Riahi et al., 2017). The SSPs provide a framework to describe alternative socio-economic developments between and within countries, which has five scenarios including sustainable pathway (SSP1), middle pathway (SSP2), regional rivalry pathway (SSP3), divided pathway (SSP4), fossil-fueled development pathway (SSP5) respectively. For the analysis of socioeconomic and climate systems, this study combines SSP and RCP (Reprehensive concentration pathways) to form a set of future global change scenarios determined by socioeconomics, emissions, climate response and anthropogenic forcing of climate system, which makes future scenarios more reasonable for the social development (O'Neill et al., 2016). Three combined SSP-RCP scenarios are selected in this study for future wheat overwintering indices in model prediction: 1) a low forcing and sustainability pathway (SSP1-2.6), which represents the combined scenario of a lower challenge of mitigation with the low radiation forcing which peaks at 2.6 W/m^2 by 2100. 2) a new forcing scenario (SSP3-7.0), which represents a combination of high social vulnerability and relatively high radiative forcing which stabilizes at 7.0 W/m^2 by 2100, and 3) a high forcing scenario (SSP5-8.5), which represents a highly energy-intensive socio-economic development pathway, whereby radiative forcing reaches 8.5 W/m2 by 2100.

Climate scenario data for 2021–2051 and historical data for 1961–1991 were provided by the Inter-Sectoral Impact Model Intercomparison Project (ISI–MIP; https://data.isimip.org/search/tree/ISIMIP3b/). The data included five climate model simulation outputs: GFDL-ESM4 (NOAA-GFDL), UKESM1-0-LL (MOHC), MPI-ESM1-2-HR (MPI-M), IPSL-CM6A-LR (IPSL), and MRI-ESM2-0 (MRI), which have been bias-corrected based on the raw data from the five aforementioned Coupled Model Intercomparison Project (CMIP6) models. The monthly mean variability of the simulated data was modified to match the observed data to preserve the long-term absolute or relative trend of the simulated data. Afterward, these data were bi-linearly interpolated in space to a $0.5° \times 0.5°$ grid (Hempel et al., 2013). In this study, a multi-model ensemble (MME) analysis of meteorological conditions related to wheat overwintering is performed based on the five climate models mentioned above.

2.3. Methodology

In the North Winter Wheat Area, whether the winter wheat can be grown safely or not is determined by the climate condition during the winter, and thus, four critical indices with significant effects on winter wheat safe planting boundaries are used here: 1) the percentage of extreme minimum temperature years occurrence, 2) the first day of the overwintering period, 3) the sowing date, and 4) the precipitation before overwintering. The percentage of extreme minimum temperature years occurrence determines whether winter wheat can resist freezing injury in the severe winter. The first day of the overwintering period and sowing date both account for the accumulated temperature of winter wheat prior to overwintering stage, as well as its overwintering ability; if the

accumulated temperature between sowing and overwintering is too low or high, the weak wheat seedling may encounter difficulties to survive through winter. And the precipitation before overwintering influences the strength of the wheat seedlings before entering the overwintering stage. It is difficult to determine the specific sowing date due to complex factors such as wheat variety and terrain (e.g., mountain area microclimates). However, the accumulated temperature from sowing date to the overwinter period must reach a certain temperature requirement (e.g., 450, 550, 700 °C) to ensure winter wheat seedling survival during the winter. Thus, the method for calculating the sowing date by required accumulative temperature is employed in this study. It is also worth noting that the accumulative temperature was calculated until December 31st over the south region of the whole winter wheat area, where no obvious overwintering period is observed. The calculations of the four indices were performed as follows:

i) Percentage of extreme minimum temperature (−22ºC) years occurred (POEMTY) in a given period:

$$POEMTY = \sum_{k=1}^{ty} I\left\{\text{tmin}_k \leq -22\right\}/ty \quad (1)$$

where ty is the total years of a study period, tmin_k is the daily minimum temperature for a certain year k, and I is a sign function, which is 1 if tmin_k is lower than or equal to −22ºC, the specified −22 °C is the lowest temperature that winter wheat can endure safely through the winter (Cooperative Agricultural and Forest Crop Regionalization Group in China, 1987; Jin, 1996).

ii) First day of the overwintering period (FD): This parameter was defined as the first day at which the daily mean temperature (i.e., based on a 5-day moving average) was below 0 °C (Wang, 1982).

iii) Sowing date (SD): the date when the cumulative temperature reaches Ta, calculating back from the FD. And Ta (i.e., 450, 550, 700 °C) is positive accumulated temperature calculation for daily average temperature greater than 0 before overwintering, according to the method described by Cui et al. (2008)

iv) Precipitation before overwintering (PBW): Total precipitation from the SD to FD

For each grid, the FD and SD are determined with an 80% guarantee rate (i.e., an agricultural climate criterion) and the PBW was calculated via the mean value over the referenced period and forecasting period.

3. Results

3.1. Percentage of extreme minimum temperature (−22ºC) years occurrence

The lowest critical temperature for winter wheat cultivation in the regions near the north boundary (along the Great Wall) has been demonstrated to be −22 °C (Jin, 1996). Therefore, POEMTY is among the most important indices to reflect climatic conditions during the winter wheat overwintering period, which directly

impacts seedling survival rate. Figure 2 illustrates the spatial distribution of POEMTY for the 1961–1990 and the 2021–2050 under SSP1-2.6, SSP3-7.0, and SSP5-8.5 scenarios. The POEMTYs were mainly concentrated in 0–20% and 80–100% intervals, and the 0% areas were marked with white lattices in Figure 2, where no lower than −22 °C extreme minimum temperature occurred. However, values of POEMTY above 50% have cold injury risk for agriculture, and farmers would no longer choose these areas to plant winter wheat. Therefore, colored areas with above 50% of POEMTY were defined as high-risk region for winter wheat growing, and low-risk (0 < POEMTY 20%) and medium-risk regions (20% < POEMTY 50%) were also defined in Figure 2. Particularly, the medium-risk region was considered as the potential extended winter wheat area along the northern boundary.

During the historical period 1961–1990 (Figure 2a), the POEMTY in the North winter wheat area was below 20%, where can meet the 80% assurance rate of guaranteed minimum temperature. In fact, the potential winter wheat planting area northern boundary was further north than the current boundary in the eastern and western portions of the North winter wheat area. At the end of the 20^{th} century, the experiments of winter wheat northward migration have been successfully carried out in Liaoning Province and Inner Mongolia (Hao et al., 2001).

During the 2021−2050, the potential safe overwintering areas for winter wheat were projected to expand under the SSP1-2.6, SSP3-7.0, and SSP5-8.5 scenarios compared to the 1961−1990 period (Figure b-d), and the high-risk area will move northwardly due to the intended climate warming. Under the SSP1-2.6 scenario, the safe overwintering areas for winter wheat will increase by 11.8% relative to 1961-1990. The risk-free area will increase by 24.7% and the wheat in 94.5% of the current North winter wheat area will no longer experience extremely low temperatures. The northern boundary of the potential planting area in Northeastern China (i.e., the eastern region) will extend to the western part of Jilin Province, and the boundary in Central Inner Mongolia (i.e., the western region) will move slightly north as well. The western part of the northern boundary could move northwardly on average by approximately 73 km and the northernmost tip of the eastern region could move 111 km northward. Under the SSP-3-7.0 scenario, the low-risk area will increase by 14.7%, and the potential northern planting boundary will move northwardly by approximately 94 km on average in the western region and by 152 km in the northernmost tip of the eastern region. Moreover, 99.0% of the current North winter wheat area will no longer experience extreme low temperatures, and the risk-free area will increase by 32.5%. Under the SSP5-8.5 scenario, the area for safe wheat overwintering will have an increase of 16.6%, the risk-free area will increase by 34.8% and the northern boundaries in the western and eastern regions will both substantially move to the north (i.e., 114 and 158 km, respectively).

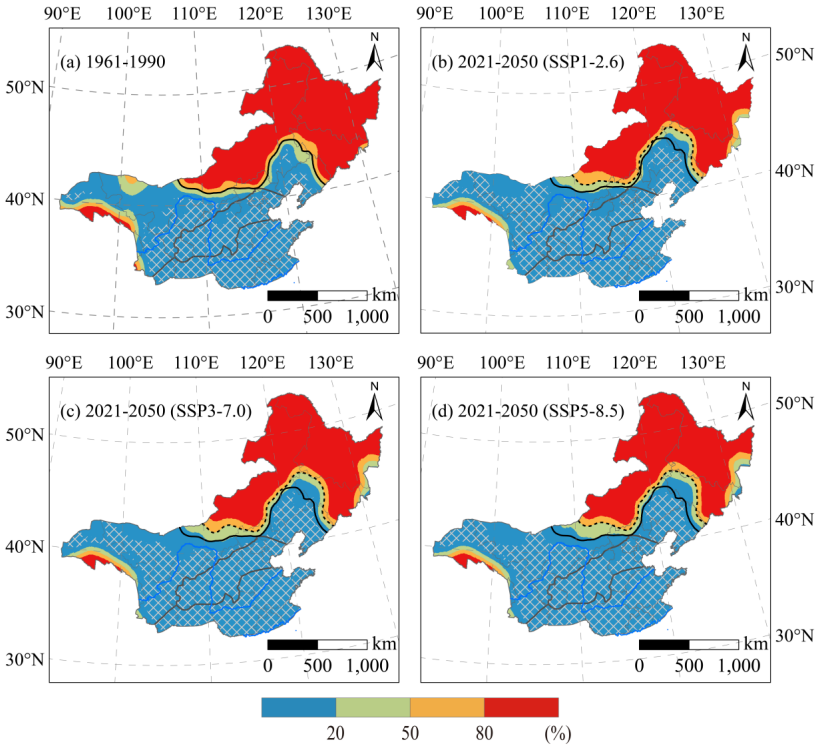

Figure 2. Spatial distribution of POEMTYs for the 1961–1990 and the 2021–2050. (a) Historical period, (b) SSP1-2.6, (c) SSP3-7.0, and (d) SSP5-8.5 scenarios. White lattices indicate that no extreme minimum temperature −22 °C occurred. The black solid and dotted lines represent the northern boundary of winter wheat cultivation in the 1961–1990 and 2021–2050 periods, respectively.

3.2. First day of the overwintering period

During the 1961–1990 reference period (Figure 3a), the FD in most part of the North winter wheat area ranged from mid-November to late December, while moving from north to south along the latitudinal gradient. In the spring wheat area, the FD occurred in early November in the southern regions of northeastern China and western Inner Mongolia, and in October in the northern and western regions of northeastern China. However, most of the northern parts of the spring wheat area were unsuitable for growing winter wheat due to the low-temperature limitations mentioned in section 3.1. The FD was from early November to early December in the northern winter wheat subregion and concentrated in mid-to-late December in Huang-Huai winter wheat subregion. However, some areas

along the Huaihe River in the southernmost part of the Huang-Huai winter wheat subregion did not exhibit noticeable overwintering periods because they are in the temperate-subtropical transition region, which is represented with dark grey dots in Figure 3a.

During the period of 2021–2050, the FD exhibited a relatively consistent spatial distribution under the three SSP-RCP scenarios, albeit with delays towards late November and later (Figure 3b-d). Taking the SSP1-2.6 scenario as an example, the winter wheat in the spring wheat area will enter the overwintering period as early as in early October, and the boundaries of the overwintering periods will move northwardly. Moreover, the largest changes will occur between late October to mid-November in northeastern China and from early- to mid-November in western Inner Mongolia. In the Northern winter wheat subregion, the FD will range from mid-November to late December from north to south. Specifically, it is mainly from mid-November to early December in the western high elevations and from mid-November to late December in the east. Winter wheat will begin to enter the overwintering period in early and mid-December in the western regions, and in late-December and later in most of the eastern plains. There will be no obvious overwintering periods in south part of the Huang-Huai winter wheat subregion, and the areas without obvious overwintering periods will increase and account for approximately 36.7%, 37.0%, and 39.7% in the Huang-Huai winter wheat subregion under the SSP1-2.6, SSP3-7.0, and SSP5-8.5 scenarios, respectively, and will be mainly distributed in some of the southern provinces, such as Shandong, Henan, Jiangsu, and Anhui, which will cause the southern boundaries of the North winter wheat area to move approximately 213, 215, and 233 km to the north (i.e., as determined by the SSP1-2.6, SSP3-7.0, and SSP5-8.5 scenarios, respectively). Compared with the reference period, the FD is delayed by 6.0, 6.6, and 7.1 days in the spring wheat area; by 8.9, 7.7, and 10.4 days in the Northern winter wheat subregion; and by 10.5, 9.0, and 10.3 days in the Huang-Huai winter wheat subregion under the SSP1-2.6, SSP3-7.0, and SSP5-8.5 scenarios, respectively. Importantly, the MME projects higher temperatures for more than half of the days from overwintering periods in 63.0% of the grids over the North winter wheat area under the SSP1-2.6 scenario compared to the SSP3-7.0 scenario. Therefore, the changing trends of some overwintering meteorological indices in this region are larger under the SSP1-2.6 scenario, such as the area without obvious overwintering periods and the FD delays.

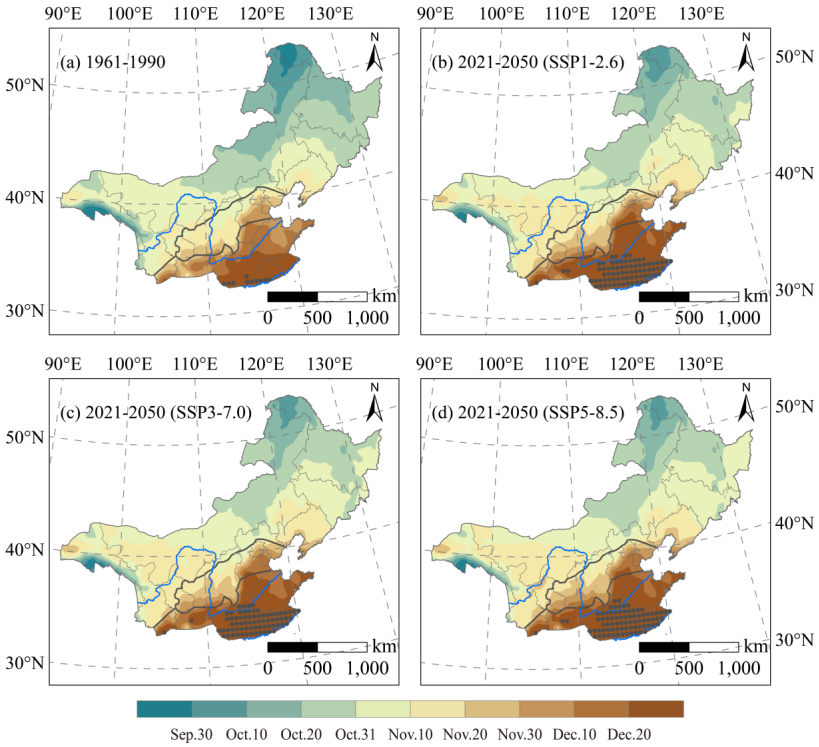

Figure 3. Spatial distribution of FDs for the 1961–1990 and 2021–2050. (a) Historical period, (b) SSP1-2.6, (c) SSP3-7.0, and (d) SSP5-8.5 scenarios. Dark grey dots indicate that there are no obvious overwintering periods in the corresponding grid points.

3.3. Sowing date

The accumulated temperature (AT) before entering the overwinter period was important factor affecting the ability of winter wheat to resist freezing conditions, and the SD in this study was calculated when the pre-winter positive accumulated temperature reached a certain value. According to previous studies (Li et al., 2013), the AT for viable seedlings was approximately 570–720 °C, and the lower limit for safe wheat overwintering was approximately 420 °C. However, wheat seedlings tended to overgrow before the winter if AT was excessive, which also led to decreases in cold resistance ability. In this study, values of 450, 550, and 700 °C were used as references to analyze SD changes in the North winter wheat area.

Figure 4 illustrates the spatial distribution features of SD during the 1961–1990

historical period, as well as under the SSP1-2.6, SSP3-7.0, and SSP5-8.5 scenarios in 2021–2050 with AT values of 450, 550, and 700 °C. The SD exhibited a gradually-delayed spatial distribution pattern from south to north but occurred earlier if the AT increased for each scenario. In the 1961–1990, when the AT was 450 °C, the SD started in mid-September and earlier in the spring wheat area, in August in the Greater Khingan Mountains and Lesser Khingan Mountains, and in mid-September in the southern regions of the Northeast Plain and western regions of Inner Mongolia. The SD was from mid-September to early-October in the west of the Taihang Mountain, the Qinling Mountain area, the Liaoning, and the northern regions of the North China Plain, mid-October in the lower and middle reaches of the Yellow River, and late October in the southern regions of the North China Plain. The SD spatial distributions for values of 550 and 700 °C were similar to those for 450 °C; however, the SD advanced as AT requirements increased, as illustrated in Figure 4 a2 and a3. Additionally, the SDs of different regions changed at varying degrees over the 1961–1990 period, exhibiting average delays of 0.3–0.4 days/decade in the spring wheat area, 0.8–0.9 days/decade in the Northern winter wheat subregion, 0.6–0.8 days/decade in the Huang-Huai winter wheat subregion, and 0.7–0.8days/decade in the entire north winter wheat area.

During the period of 2021–2050, the SDs exhibited relatively consistent spatial distributions under the three emissions scenarios for 450, 550, and 700 °C, and all showed delayed dates comparing with 1961-1990. For example, when the AT reaches 450 °C under the SSP1-2.6 scenario, the SDs are delayed from mid and late August in the reference period to late August and early September in most areas of the Greater Khingan Mountains and the Lesser Khingan Mountains, and from early-mid September to mid-to-late September in the northern boundary and its surrounding areas. In the Northern winter wheat subregion, the SDs range from mid-September and early October to late September and early October in the western regions and concentrate on early and mid-October in the eastern regions. In the Huang-Huai winter wheat subregion, the SDs are delayed from late September and early October to early and mid-October in the areas surrounding Qinling Mountain, and from late October to November in the areas along the Huaihe River. On average, the SD is delayed by 8.1 days in the spring wheat area, 7.5 days in the Northern winter wheat subregion, and 8.7 days in the Huang-Huai winter wheat subregion. For the AT of 550 and 700 °C, the SD spatial distributions are shown in Figure 4b2 and b3, with a delay of 7.7–8.8 days and 7.8–8.9 days for the three sub-districts. The SD would be further delayed under the SSP3-7.0 and SSP5-8.5 scenarios, with an average delay of 7.5 (450 °C) to 8.0 (700 °C) days for SSP3-7.0, and 8.8 (450 °C) to 9.1 (700 °C) days for SSP5-8.5 across the entire North winter wheat area. Furthermore, the SD trends over a given region are similar for different AT requirements under the same emission scenario over the predicted 2021–2050 period and the SD delay rate accelerated for all conditions compared to 1961–1990. The SDs under SSP1-2.6, SSP3-7.0, and SSP5-8.5 were respectively delayed by 1.3–1.4, 1.6–1.7, and 2.2–2.4 days/decade on average for the entire north winter wheat

area, suggesting that the impact is greater under higher emission scenarios.

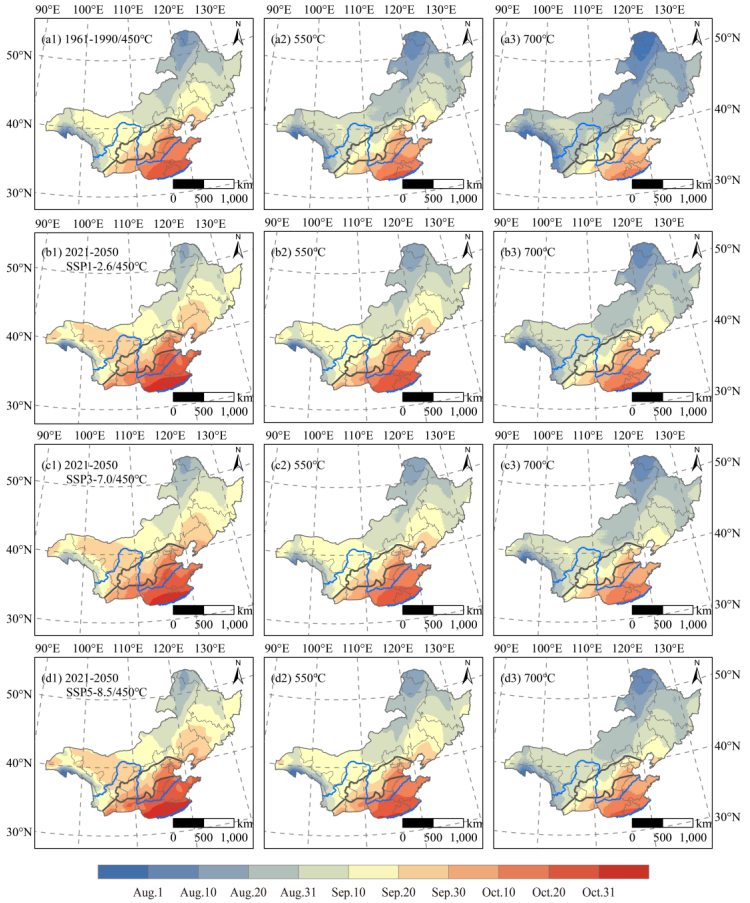

Figure 4. Spatial distribution of SD in the 1961–1990 and 2021–2050 for accumulated temperature before overwintering period at 450, 550, and 700 °C. (a1–a3) historical period, (b1–b3) SSP1-2.6, (c1–c3) SSP3-7.0, and (d1-d3) SSP5-8.5 scenarios.

3.4. Precipitation before winter

The historical spatial distribution features of PBW in 1961–1990, as well as in 2021–2050 under the SSP1-2.6, SSP3-7.0, and SSP5-8.5 radiative forcing scenarios are illustrated with AT values of 450, 550, and 700 °C (Figure 5). During the 1961–1990 reference period, when the AT was 450 °C, PBW reached more than 60 mm at the northern part of Greater Khingan Mountains, the Lesser Khingan Mountains, Changbai Mountain, and Qinling Mountain, which was followed by 40–60 mm in Taihang Mountain and the Huaihe River area, and 20–40 mm in the Northeast Plain and North China Plain. The PBW in the plateau regions west of Taihang Mountain was generally less than 60 mm

and decreased from east to west. Moreover, there was an increase in PBW with higher AT, especially at high altitudes. For example, at 700 °C of AT, the PBW was generally above 100 mm in the Greater Khingan Mountains, Lesser Khingan Mountain, Changbai Mountain, and Qinling Mountain regions; 60–80 mm in the Taihang Mountain area; 20–80 mm in the Northeast Plain and Northern China Plain; and 80–100 mm in the areas along Huaihe River.

During the period of 2021–2050, the PBWs in most areas of the North winter wheat area show a decreasing trend relative to the reference period under the SSP1-2.6, SSP3-7.0, and SSP5-8.5 scenarios. No substantial differences were observed between the spatial distribution pattern of PBW for different emissions scenarios and AT requirements. When the AT reached 450 °C under the SSP1-2.6 scenario, the regions with more than 60 mm of PBW almost reached the Greater Khingan Mountains, Lesser Khingan Mountains, and Changbai Mountain, while the western regions of Inner Mongolia received little precipitation. The western regions of the Northern winter wheat subregion exhibited more precipitation than the eastern regions, with 40–60mm and less than 40 mm of PBW, respectively. The PBWs in most regions of the Huang-Huai winter wheat subregion only received 20–40 mm, but the area near the Qinling Mountain exceeded 40 mm. On average, the PBW decreased by 13.8% in the spring wheat area, 13.7% in the Northern winter wheat subregion, and 26.7% in the Huang-Huai winter wheat subregion, relative to the reference period. For AT values of 550 and 700 °C, the PBW spatial distributions are illustrated in Fig.5b2 and b3, with 13.1–24.8% and 10.1–22.6% decreases for the three sub-districts. The PBWs would still decrease with larger reductions under the SSP5-8.5 scenario than under the SSP1-2.6 and SSP3-7.0 scenarios, which indicated that the issue of water deficiency during the historical period still intractable (Gao et al., 2019), development and management of irrigation facilities may be paid more attention over this region (Yang et al., 2022).

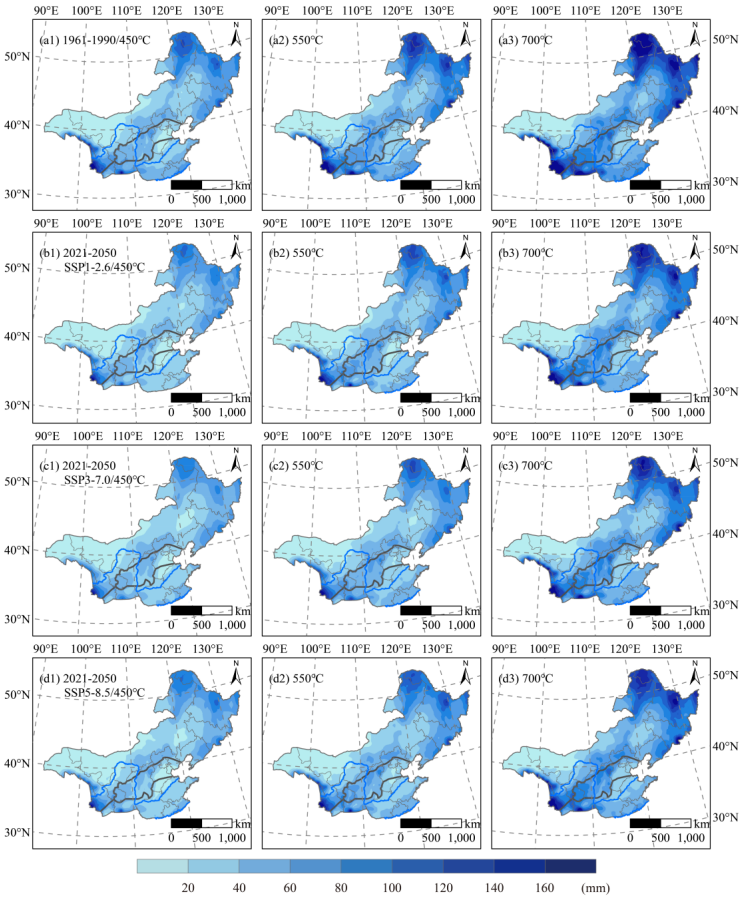

Figure 5. Spatial distribution of PBW in the 1961–1990 and 2021–2050 for accumulated temperature before overwintering period at 450, 550, and 700 °C. (a1–a3) historical scenario, (b1–b3) SSP1-2.6, (c1–c3) SSP3-7.0, and (d1-d3) SSP5-8.5 scenarios.

3.5 Planting boundaries under the different scenarios

Based on above analysis from 3.1 to 3.4, the safe planting areas are illustrated in Figure 6 for each scenario. The western region (west of 115°E) of the potential northern planting boundaries will move northwardly by approximately73, 94, and 114 km on average under the SSP1-2.6, SSP3-7.0, and SSP5-8.5 scenarios, and the northernmost tip of the eastern part will move northwardly by 111, 152, and 158 km. Due to climate change, almost 40% the Huang-Huai winter wheat subregion (i.e., 36.7%, 37.0%, and 39.7% under the three radiative forcing scenarios) will exhibit no obvious overwintering periods, causing the southern boundaries of the North winter wheat area to retract approximately 213, 215, and 233 km to the north. This indicates that some provinces in southern North

winter wheat area, such as Shandong, Henan, Jiangsu, and Anhui, would become unsuitable for winter wheat cultivation. However, the potential planting areas of the entire North winter wheat area will increase by 10.7 and 28.0 thousand km^2 on average in the SSP3-7.0 and SSP5-8.5 scenarios and decrease 38.1 thousand km^2 in the SSP1-2.6 scenario. It is worth noting that although the radiative forcing of SSP3-7.0 is higher than that of SSP1-2.6, obvious warming of SSP3-7.0 exists regional difference.

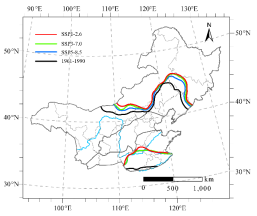

Figure 6. The possible northern and southern planting boundaries for the North Winter Wheat Area for 1961–1990 and 2021–2050 (SSP1-2.6, SSP3-7.0, and SSP5-8.5 scenarios).

4. Discussion

Winter wheat is generally planted in China due to its broad climatic adaptability, and the distribution of its cultivation zones has become the focus of a growing number of scientists to maintain high and stable yields. Previous studies mainly focused on the northward displacement of the northern planting boundary (Hao et al., 2001; Zou et al., 2001; Li et al., 2013). However, we predicted that areas with no obvious overwintering periods would experience a significant increase within the Huang-Huai winter wheat subregion, reaching the Yellow River. This indicates that most of the Huang-Huai winter wheat subregion will no longer be suitable for the currently cultivated winter wheat variety in the future. It is also worth noting that when'extreme spring cold spells' (ESCSs), occurs in northern China, continuous negative temperature anomalies can have a catastrophic impact on wheat yields, which results in yield losses of up to 20% or more. Without an overwintering period, winter wheat will likely grow excessively fast during the winter and subsequently encounter difficulties to resist cold injury in the early spring. We assumed that ESCS will occur when the daily temperature remains at least 3°C lower than the climatological daily

mean during 5 consecutive days and analyzed the probability of ESCS in the area with no obvious overwintering periods. We found that the probability of ESCS will increase from 12.5% in the 1961-1990 to 20.5%-25.5% in the forecast period (i.e., 25.5%, 20.5%, and 21.1% under the three scenarios). Additionally, plant diseases and insect pests may increase as well due to the climate change, which would further reduce winter wheat yields. Climate change also impacts the winter wheat sowing date. Here, we found that the sowing date was delayed by 0.7–0.8 days/decade on average for the entire north winter wheat area in 1961–1990. Similar results were found in some previous studies; for instance, Xiao et al. (2013) observed 1.5 days/decade average delays in the North China Plain during the 1981–2009 period. However, Liu et al. (2018) reported a larger value (3.1 days/decade) for the same period. These large variations in sowing date delays were largely due to differences in study areas and data sources. Nonetheless, our study determined that sowing dates will be delayed by 1.1–1.3, 1.9–2.0, and 2.2–2.4 days/decade in 2021–2050 under the SSP1-2.6, SSP3-7.0, and SSP5-8.5 scenarios, suggesting that the sowing date delay rate will further increase in the coming three decades.

In order to predict the northern winter wheat planting boundary, we mainly focused on whether winter wheat could safely survive the winter conditions, and calculated an index based on the minimum temperature that could be tolerated by winter wheat. However, this threshold (–22 °C) was established for the winter wheat variety in 1980, and current varieties are known to tolerate lower temperatures. For example, the strong winter wheat varieties "Dongnong winter wheat No.1," which was introduced and bred in Heilongjiang Province, can withstand a minimum temperature range of –30 to –35 °C (Wang et al., 2009). Considering that the winter wheat varieties planted in most areas of the North winter wheat area do not have such a strong resistance to freezing temperatures, this study still conservatively assumed a –22 °C minimum temperature in the winter wheat cultivation northern boundary.

Climate change plays an important role in the distribution of suitable winter wheat cultivation zones in China. This study analyzed the changes of potential winter wheat planting areas in the North winter wheat area from a strict meteorological perspective. However, our results do not necessarily imply that winter wheat can be grown in any area where the meteorological conditions are favorable, as local soil conditions, productivity levels, and agricultural policies are also critical factors that determine the suitability of a region for winter wheat cultivation. Additionally, farmers may adjust to the local conditions by choosing the correct sowing depth, adjusting the sowing date, improving crop varieties, and expanding irrigation infrastructure, all of which may lead to further variations in the actual planting boundaries for winter wheat, relative to the meteorological boundaries. Furthermore, farmers will no longer engage in production activities in areas where winter wheat planting has failed repeatedly. As a result, wheat cultivation in the northern boundary has changed very little since 2000 to reduce or avoid climate risks. Nonetheless, the winter wheat meteorological boundary is still an important reference boundary for the exploration

of new winter wheat cultivation areas, as winter wheat would be difficult to produce profitably beyond these boundaries. Therefore, actual changes in winter wheat cultivation areas should be considered comprehensively in combination with regional meteorological conditions and human activities in future studies.

5. Conclusion

This study predicted the potential changes in the northern and southern winter wheat cultivation boundaries during 2021–2050 under the SSP1-2.6, SSP3-7.0, and SSP5-8.5 radiative forcing scenarios in the North winter wheat area and its spring wheat area. The findings of this study indicate that the occurrence of extremely low-temperature years will decline in the North winter wheat area due to climate change, which will result in an increase in the potential safe overwintering areas for winter wheat cultivation in 2021–2050 by 11.8%, 14.7%, and 16.6% under the SSP1-2.6, SSP3-7.0, and SSP5-8.5 scenarios compared to the 1961–1990 reference period. The north boundary will move 0.8-1.3° northwardly on average, and the south boundary will retract 1.9-2.1° in latitude.

SD and FD, the two phenological stages before winter, are projected to be delayed in the forecasted period. Compared with the 1961–1990 reference period, the SD is delayed by 8.2–8.5, 7.5–8.0, and 8.8–9.1days, and FD is delayed by 9.9, 8.5, and 10.3 days in the entire north winter wheat area under the SSP1-2.6, SSP3-7.0, and SSP5-8.5 scenarios. Moreover, PBW is projected to experience large decreases across the entire region under the three scenarios, especially in the Huang-Huai winter wheat subregion, with reduction rates above 20%. This increases the likelihood that the southern winter wheat cultivation boundary will recede northwardly.

Acknowledgments

This study was funded by National Natural Science Foundation China (42171030, 41831174) and the Strategic Pilot Project of Chinese Academy of Sciences (XDA20020202).

Data Availability Statement

We are grateful for the maximum temperature, minimum temperature, and precipitation data for the historical and SSPs scenarios provided by NOAA-GFDL, MOHC, MPI-M, IPSL, MRI, which we downloaded at https://data.isimip.org/search/page/3/tree/ISIMIP3b/time_step/daily/climate_variable/pr/climate_variabl esm4/climate_forcing/ipsl-cm6a-lr/climate_forcing/mpi-esm1-2-hr/climate_forcing/mri-esm2-0/climate_forcing/ukesm1-0-ll/. Daily meteorological dataset of basic meteorological elements of China National Surface Weather Station (V3.0) were obtained from http://101.200.76.197/data/detail/dataCode/SURF_CLI_CHN_MUL_DAY_V3.0.html.

Declaration of competing interest

The authors declare that they have no known competing financial interests or personal relationships that could have appeared to influence the work reported in this paper.

References

Audsley, E., Pearn, K., Simota, C., Cojocaru, G., Koutsidou, E., Rounsevell, M.D.A., Trnka, M., &Alexandrov, V. (2006). What can scenario modelling tell us about future European scale agricultural land use, and what not? Environ Sci Policy. 9: 148-162.

Balkovic, J., van der Velde M., Skalsky, R., Xiong, W., Folberth, C., Khabarov, N., Smirnov, A., &Mueller, N., Obersteiner, M. (2014). Global wheat production potentials and management flexibility under the representative concentration pathways. Global Planet Change. 122: 107–121.

Cooperative Agricultural and Forest Crop Regionalization Group in China. (1987). Agricultural and Forest Crop Climate Regionalization in China. China Meteorological Press, Beijing. (in Chinese)

Cui, Y., Han, J., Cao, G., Jiang, M., &Zhang J., (2008). Effect of per-winter positive accumulated temperature on suitable planting dates of winter wheat in south centre area of Hebei. Chin Sci Bull. 24: 195–198 [in Chinese].

Gao, J., Yang, X., Zheng, B., Liu, Z., Zhao, J., Sun, S., Li, K., & Dong, C. (2019). Effects of climate change on the extension of the potential double cropping region and crop water requirements in Northern China. Agricultural and Forest Meteorology. 268: 146-155

Guo, W., Shi, H., Ma, J., Zhang, Y., Wang, J., Shu, W., &Zhang, Z. (2013). Basic Features of Climate Change in North China during 1961–2010. Adv Climate Change Res. 4: 73-83.

Hao, Z., Geng, X., Wang, F., &Zheng, J. (2018). Impacts of climate change on agrometeorological indices at winter wheat overwintering stage in northern China during 2021–2050. Int J Climatol. 38: 5576-5588.

Hao, Z., Zheng, J., & Tao, X. (2001). A study on northern boundary of winter wheat during climate warming: a case study in Liaoning Province. Prog Geogr. 20: 254–261 [in Chinese].

Hempel, S., Frieler, K., Warszawski, L., Schewe, J., & Piontek, F. (2013). A trend-preserving bias correction—the ISI-MIP approach. Earth Syst Dynam, 4: 219–236.

Hu, Q., Ma, X., Pan, X., &Huang, B. (2019). Climate Warming Changed the Planting Boundaries of Varieties of Summer Corn with Different Maturity Levels in the North China Plain. Journal of Applied Meteorology and Climatology. 12: 2605-2615

IPCC, (2021). Summary for Policymakers. In: Masson-Delmotte, V., Zhai, P., Pirani, A., Connors, S.L., Péan, C., Berger, S., Caud, N., Chen, Y., Goldfarb, L., Gomis, M.I., Huang, M., Leitzell, K., Lonnoy, E., Matthews, J.B.R., Maycock, T.K., Waterfield, T., Yelekçi, O., Yu, R., &Zhou, B. Climate Change 2021: The

Physical Science Basis. Contribution of Working Group I to the Sixth Assessment Report of the Intergovernmental Panel on Climate Change. Cambridge University Press, Cambridge, United Kingdom and New York, NY, USA.

Jin, S. (1996). Wheat Science in China. China Agriculture Press, Beijing, China [in Chinese].

Kenny, G., Harrison, P., Olesen, J., &Parry, M., 1993. The effects of climate change on land suitability of grain maize, winter wheat and cauliflower in Europe. Eur J Agron. 2: 325–338.

Li ,Y., Liang, H., &Wang, P. (2013). Effects of climate warming on the planting boundary and development stages of winter wheat. J Triticeae Crops. 33: 382–388 [in Chinese].

Li, J., &Lei, H. (2021).Tracking the spatio-temporal change of planting area of winter wheat-summer maize cropping system in the North China Plain during 2001–2018. Computers and Electronics in Agriculture. 187: 106222.

Li, K., Yang, X., Mu, C., Xu, H., &Chen, F. (2013). The possible effects of global warming on cropping system in China VIII-The effects of climate change on planting boundaries of different winter-spring varieties of winter wheat in China. Scientia Agric Sinica. 46: 1583-1594.

Li, Y., Liang, H., &Wang, P. (2013). Effects of Climate Warming on the Planting Boundary and Developmental Stages of Winter Wheat. Journal of Triticeae Crops. 33(2): 382-388.

Liu, Y., Chen, Q., Ge, Q., & Dai, J. (2018). Spatiotemporal differentiation of changes in wheat phenology in China under climate change from 1981 to 2010. Sci China Earth Sci. 61: 1088–1097.

National Bureau of Statistics of China, (2017). National Bureau of Statistics of China. National Data. http://data.stats.gov.cn/easyquery.htm?cn=C01.

O'Neill, B. C., Tebaldi, C., Vuuren, D. P. v., Eyring, V., Friedlingstein, P., Hurtt, G., Knutti, R., Kriegler, E., Lamarque, J.-F., &Lowe, J. (2016). The scenario model intercomparison project (ScenarioMIP) for CMIP6, Geoscientific Model Development. 9: 3461-3482.

Olesen, J., Carter, T., Díaz-Ambrona C., Fronzek, S., Heidmann, T., Hickler, T., Holt, T., Minguez, M. I., Morales, P., Palutikof, J., Quemada, M., Ruiz-Ramos, M., Rubæk, G., Sau, F., Smith, B., &Sykes M. (2007). Uncertainties in projected impacts of climate change on European agriculture and terrestrial ecosystems based on scenarios from regional climate models. Clim Change. 81: 123-143.

Riahi, K., Vuuren, D., Kriegler, E., Edmonds, J., O'Neill, B., Fujimori, S., Bauer, N., Calvin, K., Dellink,R., Fricko, O., Lutz, W., Popp, A., Cuaresma, J., KC, S., Leimbach, M., Jiang, L., Kram, T., Rao, S., Emmerling, J., Ebi, K., Hasegawa, T., Havlik, P., Humpenöder, F., Silva, L., Smith, S., Stehfest, E.,

Bosetti, V., Eom, J., Gernaat, D., Masui, T., Rogelj, J., Strefler, J., Drouet, L., Krey, V., Luderer, G., Harmsen, M., Takahashi, K., Baumstark, L., Doelman, J., Kainuma, M., Klimont, Z., Marangoni, G., Lotze-Campen, H., Obersteiner, M., Tabeau, A., & Tavoni, M. (2017). The Shared Socioeconomic Pathways and their energy, land use, and greenhouse gas emissions implications: An overview. Global Environ Chang. 42: 153-168.

Rosenberg, N. (1982). The increasing CO_2 concentration in the atmosphere and its implication on agricultural productivity. II. Effects through CO2-induced climatic change. Clim Change. 4: 239–254.

Rosenzweig, C. (1985). Potential CO_2-induced climate effects on North American wheat producing regions. Clim Change. 7: 367–389.

Rosenzweig, C., & Parry, M.(1994). Potential impacts of climate change on world food supply. Nature. 367: 133–138.

Shewry, P., &Hey, S. (2015). The contribution of wheat to human diet and health. Food Energy Secur. 4: 178–202.

Shiferaw, B., Smale, M., Braun, H., Duveiller, E., Reynolds, M., &Muricho, G. (2013). Crops that feed the world 10. Past successes and future challenges to the role played by wheat in global food security. Food Secur. 5: 291–317. https://doi.org/10.1007/s12571-013-0263-y.

Sun, J., Zhou, G., &Sui, X. (2012). Climatic suitability of the distribution of the winter wheat cultivation zone in China. Eur J Agron. 43:77–86.

Tadesse, W., Amri, A., Ogbonnaya, F. C., Sanchez-Garcia, M., Sohail, Q., &Baum, B. (2016). Wheat. 81–124. In Singh, M., Upadhyaya, H. Genetic and Genomic Resources for Grain Cereals Improvement. Academic Press, San Diego, CA. doi: 10.1016/B978-0-12-802000-5.00002-2.

United States Department of Agriculture (USDA), (2016). World Agricultural Production. Circular Series WAP. 7–16. https://downloads.usda.library.cornell.edu/usda-esmis/files/5q47rn72z/6w924c19w/44558d80d/worldag-production-07-12-2016.pdf. Accessed July 2016.

Vico, G., Hurry, V., &Weih, M. (2014). Snowed in for survival: Quantifying the risk of winter damage to overwintering field crops in northern temperate latitudes. Agric For Meteorol. 197: 65-75.

Wang, D., Zeng, Y., Mou, Y., Yu, J., &Cang, J. (2009). Research on antifreeze proteins of Dongnongdongmai 1 in high–cold area. J Triticeae Crops. 29: 823–826 [in Chinese].

Wang, S. (1982). A statistical method for the first and last date with the daily temperature steadily passing through the threshold. Meteorol Mon. 8: 29–30 [in Chinese].

Xiao, D., Tao, F., Liu, Y., Shi, W., Wang, M., Liu, G., Zhang, S., & Zhu, Z. (2013). Observed changes in winter wheat phenology in the North China Plain

for 1981-2009. Int J Biometeorol. 57: 275-285.

Yang, G., Li, S., Wang, H., &Wang, L. (2022). Study on agricultural cultivation development layout based on the matching characteristic of water and land resources in North China Plain. Agricultural Water Management. 259: 107272.

Yang, X., Liu, Z., &Chen, F. (2011). The Possible Effect of Climate Warming on Northern Limits of Cropping System and Crop Yield in China. Agricultural Sciences in China. 10: 585-594.

Zhang,W., Brandt, M., Prishchepov, A.V., Li, Z., Lyu, C., &Fensholt, R. (2021). Mapping the Dynamics of Winter Wheat in the North China Plain from Dense Landsat Time Series (1999 to 2019). Remote Sens. 13: 1170. https://doi.org/10.3390/rs13061170

Zhao, G.(2010). Study on Chinese wheat planting regionalization. J Triticeae Crops. 30: 886–895 [in Chinese].

Zheng, D., Yang, X., Minguez, M., Mu, C., He, Q., &Xia, W. (2018). Effect of freezing temperature and duration on winter survival and grain yield of winter wheat. Agric For Meteorol. 260-261: 1-8.

Zou, L., Zhang, J., Jiang, Q., Qing, Z., Wang, G., &Zhao, H. (2001). Research and development of winter wheat growing in northern region. Chin J Agrometeorol. 22: 54–58 [in Chinese].